Scientific Inquiry and Review (SIR)
Volume 1, Issue 1, October 2017
ISSN (P): 2521-2427, ISSN (E): 2521-2435
Journal DOI: https://doi.org/10.29145/sir
Issue DOI: https://doi.org/10.29145/sir/11
Homepage: https://ssc.umt.edu.pk/sir/Home.aspx

Journal QR Code:

Article: DFT-Mbj Study of Electronic and Magnetic Properties of Cubic Cecro3 Compound: An Ab-Initio Investigation

Author(s): M. Rashid
M. A. Iqbal
N. A. Noor

Online Published: October 2017

Article DOI: 10.29145/sir/11/010104

Article QR Code:

M Rashid

To cite this article: Rashid M, Iqbal MA, Noor NA. DFT-Mbi of electronic and magnetic properties of cubic cecro 3 compound: An Ab-Initio investigation. *Sci Inquiry Rev*. 2017;1(1):27–36. DOI: https://doi.org/10.29145/sir/11/010104

A publication of the
School of Science
University of Management and Technology
Lahore

DFT-Mbj Study of Electronic and Magnetic Properties of Cubic Cecro3 Compound: An Ab-Initio Investigation

Rashid, M[1]., Iqbal, M. A[2]. and Noor, N. A[3*].
[1]Department of Physics, COMSATS Institute of Information Technology, Islamabad, Pakistan

[2]Department of Physics, University of Management and Technology, Lahore, Pakistan

[*]naveedcssp@gmail.com

Abstract

By considering density functional theory (DFT) in terms of ab-initio investigation, we have explored the structural, electronic and magnetic properties of cubic $CeCrO_3$ for the first time. In order to determine the structural stability of cubic $CeCrO_3$ compound, we optimized the structure of $CeCrO_3$ in non-magnetic (NM), ferromagnetic (FM) and Anti-ferromagnetic (AFM) phases by using PBE generalized gradient approximation (GGA) functional to find the exchange-correlation potential. From structural optimization, the FM phase of $CeCrO_3$ is observed to be stable. For computing electronic and magnetic properties, the lately advanced modified Becke and Johnson local (spin) density approximation (mBJLDA) is used. Calculated band structures and density of states plots with an integer magnetic moment of 4 μB and reveal half-metallic character. In addition, s–d exchange constants ($N_0\alpha$) and p–d exchange constant ($N_0\beta$) are determined, which are in agreement with a distinctive magneto-optical experiment.

Keywords: *ab-initio calculations, cubic perovskite, half-metallic ferromagnetic, magnetic properties*

Introduction

Magneto-electric (ME) characteristic in the multi-ferroics, now a day's has become of vigorous importance, due to the existence of correlated ordering parameter of electric and magnetic components that gets so much attention for famous existing application such as sensor of magnetic field, memory elements for multiple state, spintronic and multi-range microwave devices etc [1-3]. Detail information of crystal and magnetic structure is matter of great concern for useful application. Recently, the rare-earth ortho-ferrites have been reported like $GdFeO_3$ [5] and $DyFeO_3$ [4] have been reported for ferro-electricity as well as ME coupling effects. It is very difficult to perform polarization measurement caused by high leakage current due to high Neel temperature of $RFeO_3$ (T_N^{Fe}=620–740K). At the same time as perovskite chromite $RCrO_3$ exhibits magnetic properties at lower TN values (110–280K).$RCrO_3$ (R=Sm- Gd- Tb- Er- Tm- and Y) [6,7] was reported to show signs of a fairly great electric polarization

(0.2–0.8μC/cm^2), initially, at somewhat high temperatures equivalent to the T_N of the Cr sub-system. Additionally, $LaCrO_3$, $CeCrO_3$ have the maximum T_N in $RCrO_3$ compounds, which is advantageous for device applications at room temperature [8].

Perovskite oxides get so much attention due to its effective use in gas separation membranes, solid fuel cell and piezoelectric etc. [9-14]. Lanthanide doped perovskite type oxides, for example $LnMeO_3$ (Ln: lanthanides, Me: transition metals), have been accustomed for functional inorganic materials having a inclusive diversity of applications for alkaline fuel cells electrodes [15], gas ions sensors [16] and catalysts for fast and complete oxidation/reduction of CO, NO and other hydrocarbons [17]. Various fascinating physical properties such as structural, electronic, optical and magnetic properties are inter-dependent in transition-metal oxides [18, 19]. These materials are predictable for spintronics devices effectively.

The association of magnetic and electronic played a role to develop the research in area of spintronics. Half-metallic ferromagnetism has a significant part because of its spin- polarization at the Fermi-level which is necessary for the better performance of spintronic applications [20, 21]. All these points force us to explore half-metallic ferromagnets with important magnetic moment that well-matched with existing semiconductor technology. Material similar to half-metal have a unique property to act as conductor in one direction of spin and insulator for opposite direction, therefore, it is very suitable for device applications and get attention for researcher that are working in the area of spintronic devices [22-24]. Some major examples are magnetic disk drives, magnetic tunnel junctions, magnetic hybrid technology for CMOS and magnetic sensor [25, 26], non-volatile magnetic random access memories (MRAM) [27, 28]. By getting research inspiration from de Groot et al. work, that explicate the insight of half-metallicity to compute band structure using the half-Heusler alloys NiMnSb [29]. Several research groups perform numerous experimental and computational studies on the HM ferromagnets, and many HM materials have been predicted and experimental verified [30].

$CeCrO_3$ belongs to Pm-3m (No. 221) space group and have cubic crystal structure. The atoms arrangement are as that Cr ions are placed at center of unit cell and coordinated with 6 oxygen ions, Ce ions are distributed at the corner of the cell and oxygen at center of the faces of unit cell. We have applied mBJ scheme, as introduced by Becker and Johnson (BJ) [31], as it can properly find electronic and magnetic characteristics. The structural properties of aforesaid crystals are calculated at ground state and equated with the prevalent theoretical and experimental data.

2. Method of Calculations

In this study, predicted results were obtained by carrying the Density Functional Theory (DFT), which is quantum mechanical approach that successful in predicting fundamental properties of compounds and alloys in terms of semiconducting trend. We employed DFT based full potential linearized augmented plane wave plus local orbital (FP-LAPW+lo) method within the frame work of Wien2K code [32]. In order to determine the ground state factors like lattice constant and bulk modulus, we used generalized gradient approximation (GGA) functional by considering the exchange-correlation potential suggested by Perdew, Burke, and Ernzerhof (PBE) [33]. Whereas, recently developed modified Becke-Johnson local density approximation functional (mBJLDA) [31] were used to analyze the magnetic and electronic properties. The aim of using mBJLDA potential for electronic properties is because of that exploring the improved predicting bandgap as associated with standard LDA [34] or GGA [33].

In FP-LAPW+lo method, ion cores inside non-overlapping spheres and a region of constant potential (interstitial region) are considered to the region between the spheres. In interstitial region, a plane wave expansion is used, whereas basis functions, potential and charge density were prolonged as arrangements of spherical harmonic functions. The value of lmax=10 in muffin-tin spheres for charge density and non-spherical potential was accomplished. For energy merging, basis function expand upto $R_{MT}\times K_{max}=8$ (in the plane wave extension R_{MT} represent the minimum sphere radius and K_{MAX} the amount of the largest K vector). A mesh of 56 k-points was used in the irreducible part of the Brillouin zone (BZ) for structural, magnetic and electronic properties, which certifies the convergence, are 3000 k-points. In addition, the charge density was Fourier prolonged up to $G_{max} = 16$. For cubic $CeCrO_3$ perovskites, the R_{MT} values were elected to be 2.5, 1.72 and 1.87a.u. (atomic units) for Ce, Cr and O correspondingly. For energy convergence, the calculations of self-consistent were performed iteratively, when the total energy of the system is steady within 0.01 mRy.

3. Results and Discussion

3.1. Structural properties

To understand DFT based cubic $CeCrO_3$, structure stability is check by performing structural optimization in NM, FM and AFM phases. By using GGA-PBE scheme, optimization is done by minimizing the total energy with reverence to unit cell volume in each phase. From computed results (see Figure1), the total energy difference between these two as $\Delta E = E_{NM} - E_{FM}$ and $\Delta E = E_{AFM} - E_{FM}$. The positive of ΔE confirmed that $CeCrO_3$ is stable in FM phase (see Table 1). In ABO_3 oxides with B=Mn, Cr, Fe, Ni and Co, most of such oxides have FM character. Similar, FM character is also proved in our study. Therefore, in first step, we performed optimization in FM phase to compute the lattice constant a(Å) and bulk modulus B for $CeCrO_3$are shown in Table1.

The calculated tolerance factors for $CeCrO_3$ are mentioned in Table1. Our calculated value of tolerance factor is in adjacent covenant with the calculated results [35, 36]. In cubic perovskite, the tolerance factor lies between 0.93 and 1.02 [36] and our measured values employed in this range, illuminating the cubic structure of $CeCrO_3$ compounds. The bond lengths are measured between various atoms of the $CeCrO_3$ and also listed in Table1. The tolerance factor can be calculated using bond lengths by using the consequent formula:

$$t = \frac{0.707(< Ce - O >)}{(< Cr - O >)}$$

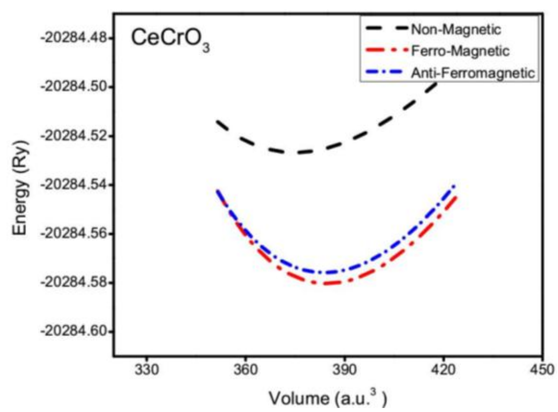

Figure1. The computed total minimum energy versus unit cell volume in non-magnetic, ferro-magnetic and anti-ferromagnetic cubic $CeCrO_3$ compound

Table1.
Calculated lattice parameters a(Å), Bulk moduli B(GPa), Tolerance factor, Bond length, bandgap Eg (eV), Half-metallic E_{HM}(eV), magnetic moments (μ_B) and exchange constant parameters of FM cubic $CeCrO_3$

Parameter	$CeCrO_3$
a_0(Å)	3.877
B_0(GPa)	183.81
Tolerance factor	0.999
Bond length Cr-O	1.9373
Bond length Ce-O	2.7397
Bond length Cr-Ce	3.355
Eg (eV)	2.89
E_{HM}(eV)	0.38

Total (μ_B)	4.0004
Cr (μ_B)	2.5283
Ce (μ_B)	0.9831
O (μ_B)	0.0642
Δx (d)	4.25
Δx (pd)	3.14
ΔE_C (eV)	0.42
ΔE_v (eV)	2.70
$N_o\alpha$	0.33
$N_o\beta$	2.14

3.2. Electronic properties

Electronic band structure with mBJ DFT studies was discussed in this electronic part. Energy eigen values obtained with the help of KS equation for Electronic band structure. In the magnetic properties of $CeCrO_3$ show match of band structure due to spin up (↑) and down (↓) orientation of FM $CeCrO_3$ polarized band structure in Figure2. In the analysis of spin-up state band structure, it will be seen that the valance band (VB) maxima and conduction band (CB) minima both found at point M of Brillion Zone (see in Figure2). For above analysis, it is seen that up spin state of $CeCrO_3$ demonstrate the FM semiconductors behavior. The VB maxima cross the Fermi level (EF) for spin down channel in $CeCrO_3$, which describe the half-metallic manners is there for spin down (↓) state. To disclose the starting point of density of states, partial density of state for $CeCrO_3$ is calculated and shown in the Figure3.

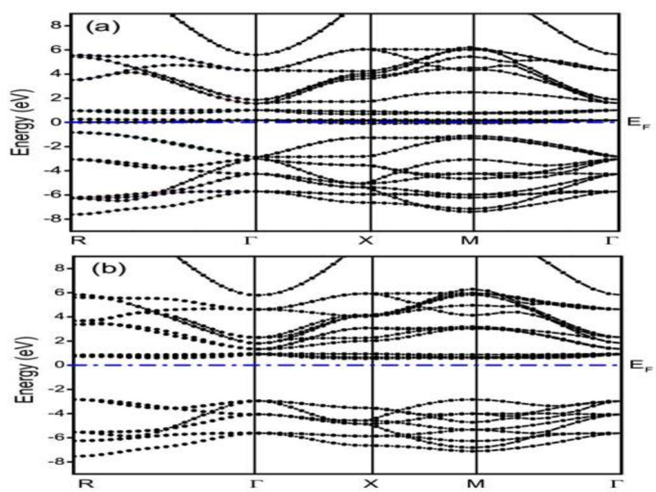

Figure2**.** The Calculated Spin Polarized Ferromagnetic Band Structures for Cubic $Cecro_3$ Compound with Mbj Potential

The (a) for majority spin (↑) and the (b) for minority spin (↓)

It understood able the Fermi level E_F is cross for spin up, total DOS, on the other hand the down channel form band gap at $E_{F,}$ resultant the charges make a complete spin polarization and form this compound to utilize it for spintronics devices. For compound $CeCrO_3$ and by means of mBJ 2*p* states and 3*d* states of O and Cr contributed primarily in the region of VB involving -4 eV to Fermi level. If we deeply analyzed DOS from E_F to 1 eV, we observed the 4*f* orbitals of Ce contribution in DOS, after active over 3*d* states of Cr is clearly depicted. The shift in these states to-words high energies and the contribution of 4*f* states of Ce increments in the region of Fermi level clues to observed p-type conductivity and 100% spin polarization.

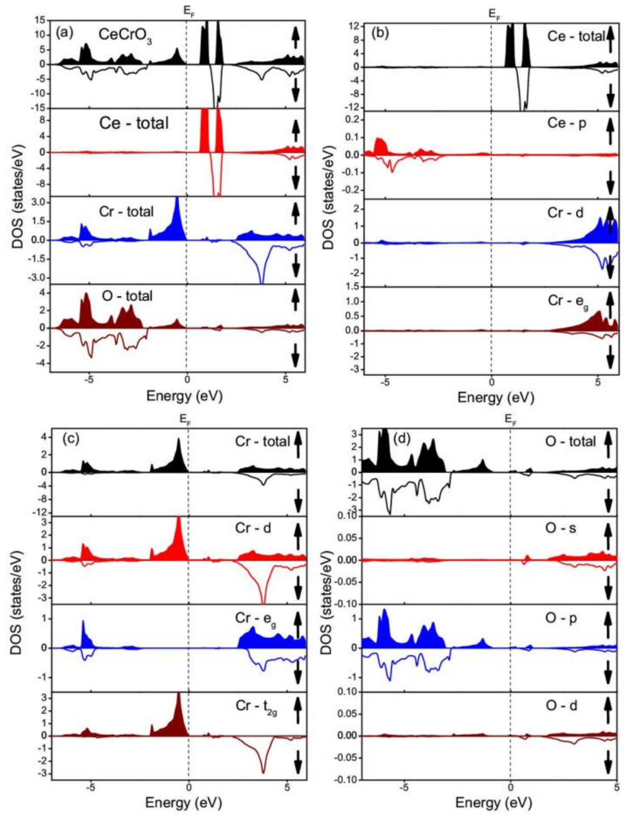

Figure3. The calculated (a) total density of states (DOS), along partial DOS of (b) Ce, (c) Cr and (d) O by using mBJ for $CeCrO_3$ compound.

3.3. Magnetic Properties

We obtained magnetic moment $CeCrO_3$ from mBJ and listed in the Table1. Although, the calculated value is to some extent lesser than the theory value (μ_{Cr}=2.52 μB). The fact of the smaller value is that the electrons in 3*d* are not totally confined but hybridized with oxygen of its 2*p* states. We have been also calculated magnetic moments of Ce ions. From the calculation we suggest that the total magnetic moment is predominantly because of Cr atoms and the M_{Ce} may be negligible. The half metallic characteristic of materials is verified by the numeral value of total magnetic moment. In our verdict the dual exchange method is liable for ferromagnetism seen in $CeCrO_3$ cubic perovskites and has indirect exchange interface among transition metals and rare-earths by the mean of anion O.

In addition splitting energy $\Delta_x(d)$ values of spin exchange that describes the role of 3*d* states of transition metal in exchange method is studied for Cr, and listed in the Table1. Most exciting calculated parameters from *p-d* and *s-d* coupling are swap coefficients $N_0\alpha$, $N_0\beta$, correspondingly [37], that decide the swap interaction among TM *d*-state as well as charge carriers (holes and electrons in the valance band and conduction band respectively). The swap coefficients values for $CeCrO_3$ are shown in Table1. Additional, the value of $N_0\alpha$ has lower than $N_0\beta$ indicate that the *s-d* contact at CB minima is greatly feebler than *p-d* interaction at VB maxima, that may be evidence of ferromagnetic behavior present in the given compound.

4. Conclusion

In conclusion, we have perceived structural, electronic and magnetic properties of FM $CeCrO_3$ compound by means of ab-initio calculations. To verify the stability of $CeCrO_3$ compound, we have optimized the structure in PM, FM and AFM phases and have computed their total energy differences (ΔE_1 and ΔE_2). The calculated value of ΔE_1 and ΔE_2 are positive, which confirm that $CeCrO_3$ is stable in FM phase. By analyzing band structure and density of state plots, we find that $CeCrO_3$ is a half-metallic ferromagnet, while predicted value of total magnetic moments is 4 μB. In addition, Cr 3*d* (unfilled) state due to *p-d* hybridization results in a fall of magnetic moment of Cr ions and identical of magnetic moment in the Ce and O (nonmagnetic) ions. Furthermore, calculated exchange constant $N_0\alpha$ and $N_0\beta$ indicate a lower value of $N_0\alpha$ than $N_0\beta$, which represents that spin-down state is more operative, due to *p-d* interaction at valance band maxima and ferromagnetism is confirmed by their strong hybridization. Furthermore, double-exchange mechanism is used to discuss the origin of the ferromagnetism in $CeCrO_3$.

References

[1] Spaldin NA, Fiebig M. The renaissance of magnetoelectric multiferroics. *Science.* 2005;309(5733):391–392.

[2] Fiebig M. Revival of the magnetoelectric effect. *J Phys D Appl Phys.* 2005;38(8):123–152.

[3] Khomskii D. Classifying multiferroics: mechanisms and effects. *Physics.* 2009;2(20):20–28.

[4] Tokunaga Y, Iguchi S, Arima T, Tokura Y. Magnetic-Field-Induced Ferroelectric State in $DyFeO_3$. *Phys Rev Lett.* 2008;101(9):097205–097210.

[5] Tokunaga Y, Furukawa N, Sakai H, Taguchi Y, Arima TH, Tokura Y. Composite domain walls in a multiferroic perovskite ferrite. *Nat Mater*. 2009;8:558–562.

[6] Rajeswaran B, Khomskii DI, Zvezdin AK, Rao, CN, Sundaresan A. Field-induced polar order at the Néel temperature of chromium in rare-earth orthochromites: Interplay of rare-earth and Cr magnetism. *Phys Rev B.* 2012;86(21):214409–214415.

[7] Serrao CR, Kundu AK, Krupanidhi SB, Waghmare UV, Rao CN. Biferroic $YCrO_3$. *Phys Rev.* 2005;B**72**:220101–220108.

[8] Zhou JS, Alonso JA, Pomjakushin V, Goodenough, JB, Ren Y, Yan JQ, et al. Intrinsic structural distortion and super exchange interaction in the orthorhombic rare-earth perovskites RCrO3. *Phys Rev B.* 2010;81(21):214115–214120.

[9] Fong DD, Stephenson GB, Streiffer SK, Eastman JA, Auciello O, Fuoss PH, et al. Ferroelectricity in ultrathin perovskite films. *Science.* 2004;304(5677):1650–1653.

[10] Petric A, Huang P, Tietz F, Evaluation of La–Sr–Co–Fe–O perovskites for solid oxide fuel cells and gas separation membranes. *Sol State Ion.* 2000;135(1–4):719–725.

[11] Pena MA, Fierro JL. Chemical Structures and performance of Perovskite Oxide. *Chem Rev.* 2000;101(7):1981–2017.

[12] Galasso FS. *Perovskites and High Tc Superconductors.* New York: Gordon and Breach; 1990.

[13] Murtaza G, Ahmad I, Amin B, Afaq A, Maqbool M, Maqsood JK, et al. Investigation of structural and optoelectronic properties of $BaThO_3$. *Opt Mater.* 2011;33(3):553–557.

[14] Hayatullah, Murtaza G, Khenata R, Mohammad S, Naeem S, Khalid MN, et al. Structural, elastic, electronic and optical properties of CsMCl3 (M=Zn, Cd). *Physica B.* 2013;420:15–23.

[15] Meadowcroft DB. Low-cost oxygen electrode material. *Nature***.** 1970;226:847–848.

[16] Yang M, Huo L, Zhao H, Gao S, Rong Z. Electrical properties and Acetone-Sensing characteristics of LaNi1–xTixO3 Perovskite System Prepared by Amorphous Citrate Decomposition. *Sens Actuators B Chem.* 2009;143(1):111–118.

[17] Zhang HM, Shimizu Y, Teraoka Y, Miura N, Yamazoe N, Oxygen sorption and catalytic properties of La1−xSrxCo1−yFeyO3 Perovskite-type oxides. *J Catal*. 1990;121(2):432–440.

[18] Wong KM, Alay-e-Abbas SM, Shaukat A, Fang Y, Lei Y. First-principles investigation of the size-dependent structural stability and electronic properties of O-vacancies at the ZnO polar and non-polar surfaces. *J Appl Phys*. 2013;113(1):014304.

[19] Wong KM, Alay-e-Abbas SM, Fang Y, Shaukat A, Lei Y. Spatial distribution of neutral oxygen vacancies on ZnO nanowire surfaces: an investigation combining confocal microscopy and first principles calculations. *J Appl Phys*. 2013;114(3):034901.

[20] Wolf SA, Awschalom DD, Buhrman RA, Daughton JM, von-Molnar S, Roukes ML, et al. Spintronics: a spin-based electronics vision for the future. *Science.* 2001;294(5546):1488–95.

[21] Pickett WE, Moodera JS. Half metallic magnets. *Phys Today*. 2001;54:39.

[22] Saeed Y, Nazir S, Shaukat A, Reshak AH. Ab-initio calculations of Co-based diluted magnetic semiconductors Cd1−xCoxX (X=S, Se, Te). *J Magn Magn Mater*. 2010;322(20):3214–3222.

[23] Nazir S, Ikram N, Siddiqi SA, Saeed Y, Shaukat A, Reshak AH. First principles density functional calculations of half-metallic ferromagnetism in Zn1-xCrxS and Cd1-xCrxS. Curr *Opin Solid State Mater Sci.* 2010;14(1):1–6.

[24] Saini HS, Singh M, Reshak AH, Kashyap MK. Emergence of half metallicity in Cr-doped GaP dilute magnetic semiconductor compound within solubility limit. *J Alloy Compd.* 2012;536:214–218.

[25] Wurmehl S, Fecher GH, Kandpal HC, Ksenofontov V, Felser C, Lin HJ. Investigation of Co2FeSi: the Heusler compound with highest Curie temperature and magnetic moment. *Appl Phys Lett.* 2006;88(3)**:**032503.

[26] Wang W, Liu E, Kodzuka M, Sukegawa H, Wojcik M, Jedryka E, et al. Coherent tunneling and giant tunneling magnetoresistance in Co2FeAl/MgO/CoFe magnetic tunneling junctions. *Phys Rev B.* 2010;81(14):140402.

[27] Zutic I, Fabian J, Das-Sarma S. Spintronics: fundamentals and applications. *Rev Mod Phys*.2004;76(2):323.

[28] Karaca M, Kervan S, Kervan N. Half-metallic ferromagnetism in the CsSe compound by density functional theory. *J Alloy Compd.* 2015;639:162–167.

[29] de Groot RA, Mueller FM, van Engen PD, Buschow KH. New Class of Materials: Half-Metallic Ferromagnets. *Phys Rev Lett.* 1983;50(25):2024.

[30] Si C, Zhou J, Sun Z, Half-Metallic ferromagnetism and surface functionalization-induced metal–insulator Transition in Graphene-like two-dimensional Cr2C crystals. *ACS Appl Mater Interfaces***.** 2015;7(31):17510–17515.

[31] Tran F, Blaha P. Accurate band gaps of semiconductors and insulators with a semi local exchange-correlation potential. *Phys Rev Lett.* 2009;102(22):226401.

[32] Blaha P, Schwarz K, Madsen G, Kvasnicka D, Luitz J. *WIEN2K: An augmented plane wave + local orbitals program for calculating crystal propertie.* Vienna, Austria: Vienna University of Technology; 2001.

[33] Perdew JP, Burke K, Ernzerhof M. Generalized gradient approximation made simple. *Phys Rev Lett.* 1997;**77**:3865.

[34] Martin RM. *Electronic structure: basic theory and practical methods.* Cambridge: Cambridge University Press; 2004.

[35] Kumar A, Verma AS, Bhardwaj SR. Prediction of Formability in Perovskite-Type Oxides. *The Open Applied Physics Journal.* 2008;1:11–19.

[36] Xu N, Zhao H, Zhou X, Wei W, Lu X, Li F. Dependence of critical radius of the cubic perovskite ABO 3 oxides on the radius of A- and B-site cations. *Int J Hydrog Energy*. 2010;35:7295–7301.

[37] Sanvito S, Ordejon P, Hill NA. First-principles study of the origin and nature of ferromagnetism in Ga1−xMnxAs. *Phys Rev B.* 2001;63(16):165206.